

How the X-ray spectrum of a Narrow-Line Seyfert 1 galaxy may be reflection dominated

A. C. Fabian^{1*}, D. R. Ballantyne¹, A. Merloni¹, S. Vaughan¹, K. Iwasawa¹ and Th. Boller²

¹*Institute of Astronomy, Madingley Road, Cambridge CB3 0HA*

²*Max-Planck-Institut für extraterrestrische Physik, Postfach 1603, 85748 Garching, Germany*

20 July 2021

ABSTRACT

A model for the inner regions of accretion flows is presented where, due to disc instabilities, cold and dense material is clumped into deep sheets or rings. Surrounding these density enhancements is hot, tenuous gas where coronal dissipation processes occur. We expect this situation to be most relevant when the accretion rate is close to Eddington and the disc is radiation-pressure dominated, and so may apply to Narrow-Line Seyfert 1 (NLS1) galaxies. In this scenario, the hard X-ray source is obscured for most observers, and so the detected X-ray emission would be dominated by reflection off the walls of the sheets. A simple Comptonization calculation shows that the large photon-indices characteristic of NLS1s would be a natural outcome of two reprocessors closely surrounding the hard X-ray source. We test this model by fitting the *XMM-Newton* spectrum of the NLS1 1H 0707–495 between 0.5 and 11 keV with reflection dominated ionized disc models. A very good fit is found with three different reflectors each subject to the same $\Gamma = 2.35$ power-law. An iron overabundance is still required to fit the sharp drop in the spectrum at around 7 keV. We note that even a small corrugation of the accretion disc may result in $\Gamma > 2$ and a strong reflection component in the observed spectrum. Therefore, this model may also explain the strength and the variability characteristics of the MCG–6-30-15 Fe $K\alpha$ line. The idea needs to be tested with further broadband *XMM-Newton* observations of NLS1s.

Key words: accretion, accretion discs – line: formation – galaxies: active – X-rays: galaxies – X-rays: general – galaxies: individual: 1H 0707–495

1 INTRODUCTION

The basic model for the active nucleus of a typical Seyfert 1 galaxy consists of a black hole surrounded by an ultraviolet and soft X-ray emitting thin accretion disc above which a patchy active corona emits hard X-rays. The model is supported by strong X-ray reflection signatures due to Compton backscattering and fluorescence of the harder coronal X-rays by the dense disk (Pounds et al. 1990; Nandra & Pounds 1994; Petrucci et al. 2000). In some objects an extreme red wing is found in the iron line of the reflection spectrum (Tanaka et al. 1995; Nandra et al. 1999; Fabian et al. 2000), showing that the disk can extend very close to the black hole where large relativistic effects occur. In general the strength of the reflection spectrum indicates that the disk surface is approximately flat, although disk instabilities could well make it ribbed or clumpy, particularly if the disk is radiation-pressure dominated (e.g., Lightman & Eardley 1974; Guilbert & Rees 1988; Krolik 1998; Turner, Stone & Sano 2001). Such a situation is most likely to occur when the accretion rate is high and close to the Eddington limit, which is often

thought to explain the unusual properties of Narrow-Line Seyfert 1 (NLS1) galaxies (e.g., Pounds, Done & Osborne 1995).

Recently, Boller et al. (2002) reported on a “sharp spectral feature” at about 7.1 keV in the *XMM-Newton* spectrum of the NLS1 1H 0707–495 ($z = 0.0411$). This deep drop (over a factor of two in flux) in the spectrum occurs at almost the exact energy of the neutral iron edge, so absorption models (in particular, a partial covering model) were favoured to explain the feature. However, these models suffered from a very soft intrinsic power-law ($\Gamma \sim 3.5$) and an unreasonably large value of the iron abundance ($\sim 35\times$ solar). Moreover, it was difficult for the partial covering model to account for the absence of a narrow Fe $K\alpha$ line and to explain the rapid variability of the source over the entire waveband. The sharp drop in the spectrum could also be due to the blue wing of a relativistic iron emission line, but, as the authors noted, to explain the depth of the drop at ~ 7 keV requires “invoking a very extreme Fe abundance and/or reflection fraction.” Here, we consider the possibility of a reflection dominated X-ray spectrum in detail.

The basic idea we wish to explore is that within a system which is accreting at close to the Eddington rate, disc instabilities funnel denser material into many deep rings, between which the hard X-rays are emitted by some coronal process (Figure 1). To

* acf@ast.cam.ac.uk

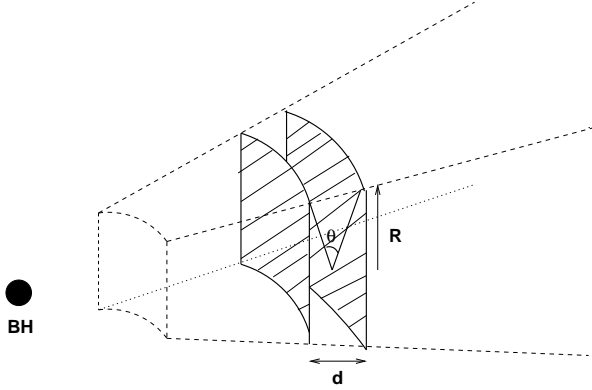


Figure 1. The proposed geometry. The inner region of the radiation-pressure dominated accretion disc is broken up into a series of deep sheets or rings, with a typical size, R , of the order of the disc thickness, and separated by a distance d . Hard X-ray sources are found in between the sheets, but are obscured from the view of observers along most line-of-sights. Therefore, the detected X-ray emission is dominated solely by the reflected emission from the walls of the sheets. In Section 2, we have considered circular sheets of radius R instead of squared ones to simplify the computations.

an off-axis observer, the X-ray emission will consist mostly of a reflection component. The rapid variability seen in the X-ray emission from 1H 0707–495 could then in part be due to changes in the geometric obscuration of one sheet on another, explaining why little spectral variability is seen (Boller et al. 2002). This reflection model requires a less extreme input spectrum and hidden flux than the partial-covering model. While this is clearly an idealized picture, recent numerical simulations of the magneto-rotational instability in radiation-pressure dominated discs have found that the turbulence can cause density contrasts up to a factor of 200 (Turner, Stone & Sano 2001). Therefore, it does seem plausible that a radiation-pressure dominated disc will exhibit strong density inhomogeneities.

In the next section, we calculate what the hard X-ray power-law may look like in our idealized picture and show that a steep spectrum naturally arises from this situation. In Section 3 we fit reflection dominated spectra to the broadband *XMM-Newton* data of 1H 0707–495. Finally, we discuss the implications of this model in Section 4.

2 CALCULATION OF THE X-RAY POWER-LAW

Here we give a simple analytic estimate of the slope of the X-ray continuum by assuming that in the inner radiation-pressure dominated part of the accretion disc the dense and cold sheet-like part of the flow is embedded in a tenuous, hot plasma (cf., Guilbert & Rees 1988; Celotti, Fabian & Rees 1992; Kuncic, Blackman & Rees 1996; Kuncic, Celotti & Rees 1997). The accretion energy is dissipated, probably via magnetic reconnection, in the hot phase only, with the cold sheets reprocessing (reflecting and thermalizing) the incident hard flux.

For ease of computation, the picture in Fig. 1 was adapted so that the cold sheets have a flat disc-like geometry with radius R .

We consider two such discs facing each other and separated by a distance d . The hot phase is sandwiched by the two cold discs and therefore has a cylindrical slab geometry. From a point in the mid-plane of the cylinder, at a distance r from its centre, the covering fraction of the two cold sheets is

$$C(r) = \left[1 - \frac{1}{2} \left(\frac{1}{\sqrt{1 + \frac{4(R-r)^2}{d^2}}} + \frac{1}{\sqrt{1 + \frac{4(R+r)^2}{d^2}}} \right) \right]. \quad (1)$$

The average total covering fraction is then given by

$$C = \frac{1}{R} \int_0^R C(r) dr = 1 - \frac{d}{4R} \left[\log \left(\frac{4R}{d} + \sqrt{1 + \frac{16R^2}{d^2}} \right) \right]. \quad (2)$$

With the hard luminosity of the hot phase being L_H , the reprocessed luminosity is given by

$$L_{\text{rep}} = CL_H(1 - a), \quad (3)$$

where a is the albedo of the cold sheets. We make use of the results of Malzac, Beloborodov & Poutanen (2001) who used Monte Carlo simulations of Comptonizing coronae above dense cold material and showed that the albedo depends on the spectral index of the illuminating radiation, being smaller for steep spectra. The thermal reprocessed soft photon flux from the cold sheets is assumed to be a black-body spectrum with temperature T_{rep} , and is calculated by the method outlined by Merloni & Fabian (2001). The hard luminosity is assumed to be due only to inverse Compton scattered photons and can be approximated as a sum of a cut-off power-law and Wien component (Wardziński & Zdziarski 2000).

The emerging spectral index of the power-law is given by

$$\Gamma - 1 = \alpha = - \frac{\ln P_{\text{sc}}}{\ln(1 + 4\Theta + 16\Theta^2)}, \quad (4)$$

where $\Theta = kT_e/m_e c^2$ is the electron temperature of the hot phase, and P_{sc} is the scattering probability averaged over the source volume and depends only on the coronal optical depth τ . In a slab geometry P_{sc} can be approximated as (Zdziarski 1994)

$$P_{\text{sc}} = 1 + \frac{\exp(-\tau)}{2} \left(\frac{1}{\tau} - 1 \right) - \frac{1}{2\tau} + \frac{\tau}{2} E_1(\tau), \quad (5)$$

where E_1 is the exponential integral.

Once the geometry is fixed (by fixing the aspect ratio R/d), the temperature of the hot phase, and consequently the slope of the Comptonized continuum, can be calculated self-consistently by solving $L_H = L_C = \int_{2.78\Theta_{\text{rep}}}^{\infty} L_C(x) dx$. We have calculated the spectral index Γ for different values of the ratio R/d and in Figure 2 we plot the spectral index for three different values of the optical depth of the hot phase. Clearly, as the covering fraction increases, the spectrum softens significantly. Also, the spectrum is steeper for a denser hot medium (larger τ). Finally, if there is accretion energy dissipated in the cold phase, then the spectrum will be softer for a given R/d (c.f., Malzac 2001).

Figure 3 shows an equivalent plot where the abscissa is now the half opening angle between the two reproducers $\theta/2$. These plots show that spectral indices typical of NLS1s (i.e., $\Gamma > 2.1$ – 2.2) are a natural consequence of this scenario if the half opening angle between the two reproducers is less than about 20 degrees. In such a case, it is likely that an observer may only detect the reflected emission arising from the walls of the reproducers.

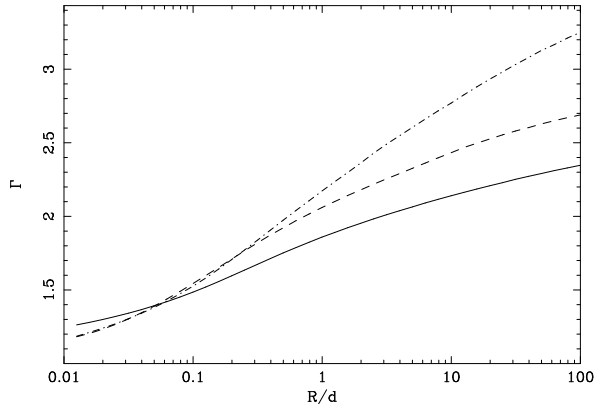


Figure 2. The spectral index Γ as a function of the aspect ratio R/d , for $\tau = 0.1$ (solid line), $\tau = 1$ (dashed line) and $\tau = 10$ (dot-dashed line).

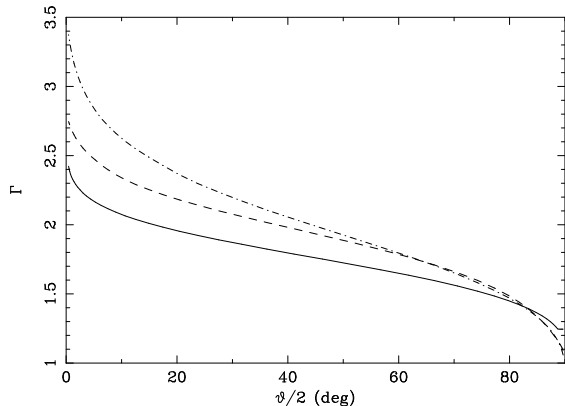


Figure 3. The spectral index Γ as a function of the half opening angle of the couple of disc-like cold sheets for $\tau = 0.1$ (solid line), $\tau = 1$ (dashed line) and $\tau = 10$ (dot-dashed line).

3 APPLICATION TO THE NLS1 1H 0707–495

In this section, we attempt to fit the broadband X-ray spectrum of the NLS1 1H 0707–495 with models of reflection dominated spectra, which might be expected if the accretion disc has broken into a number of dense segments (Fig. 1). We consider the EPIC-pn spectrum of 1H 0707–495 between 0.5 and 11 keV and fit with the constant density ionized disc models of Ross & Fabian (1993) (see also Ross, Fabian & Young 1999). The parameters of the model are the ionization parameter $\xi = 4\pi F_X/n_H$, where F_X is the illuminating flux between 10 eV and 100 keV, the photon index of the power-law spectrum that strikes the slab, and a normalization constant. Relativistic blurring was applied to the model during fitting using the kernel of Laor (1991). The emissivity index was fixed at -3 , but the inner and outer radii, along with the inclination angle, were left free. Absorption due to the Galactic column of $5.79 \times 10^{20} \text{ cm}^{-2}$ was included in all fits.

If one tries to fit the data with a single reflection spectrum, then the best fit ($\chi^2/\text{d.o.f.}=506/309$) is obtained with a model with a three times solar Fe abundance. Recall that no power-law component has been added to these models, giving them, in effect, an infinite reflection fraction. We find that $\Gamma = 2.44$ and $\log \xi = 2.040$, which results in a strong neutral Fe K α line. Extreme Kerr blurring ($r_{\text{in}} = 1.24 r_g$) was needed to fit the large red wing of the line between 2.5 and 6 keV. However, as indicated by the large χ^2 , there were significant residuals to the fit, particularly below 1 keV where

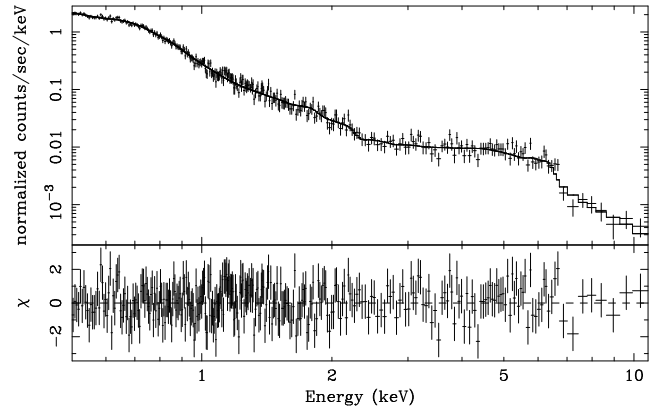


Figure 4. The upper panel shows the folded three-reflector model and EPIC-pn data of 1H 0707–495 between 0.5 and 11 keV. The lower panel displays the residuals to the fit in units of standard deviations.

the model predicts strong emission lines from Fe and O (Ross & Fabian 1993). To dilute the effect of these lines, a power-law was added to the model with the value of Γ fixed to be the same as the reflected component. Reflection still dominated the spectrum with a reflection fraction > 10 . The power-law improved the best fit to $\chi^2/\text{d.o.f.}=479/308$, but required an Fe abundance greater than 5 times solar. In this fit, Γ softened slightly to 2.52, but there was little change in the ionization parameter, the inner and outer radii, or the inclination angle (~ 23 degrees). There are still residuals below 1 keV, but, interestingly, there is now a clear line-like residual just above 6 keV. Adding a Gaussian to the fit drops the χ^2 by 38 with the addition of three degrees of freedom – significant at > 99.99 per cent, according to the F-test. Here, the best-fit model has a seven times overabundance of Fe, and $\Gamma = 2.56$. The line had an energy of 6.62 keV and a width $\sigma = 0.235$ keV, indicating that it probably also arises from somewhere in or on the disk.

To investigate this further, the power-law and Gaussian components of the model were replaced by a second reflector. The second reflection component was drawn from the same group of models as the first, and was also subject to relativistic blurring. We fixed the photon-index and inclination angle to be the same for both components. The addition of this second reflector greatly improved the fit ($\chi^2/\text{d.o.f.}=342/305$), as the combined emission removed most of the residuals from the soft X-ray band, and now only a five times overabundance of Fe was required. The ionization parameter of the second component is $\log \xi = 3.397$ resulting in a strong He-like Fe K α line at 6.7 keV and an inner radius of $5.4 r_g$. The other reflector remained relatively neutral with $\log \xi = 2.09$ and strongly blurred ($r_{\text{in}} = 1.24 r_g$). The photon-index flattened slightly to $\Gamma = 2.41$. While this fit is almost acceptable there is still a line-like residual above 6 keV. Adding a Gaussian component to account for this feature significantly improves the fit ($\chi^2/\text{d.o.f.}=292/302$). This new line has an energy of 6.45 keV and a width of 0.358 keV, demonstrating that the line arises from weakly ionized Fe in the accretion disc.

The two-reflector plus Gaussian emission line model gives a very good fit to the EPIC-pn data between 0.5 and 11 keV, however it is interesting to consider replacing the line component with a third reflection spectrum. This model also results in an excellent fit to the data ($\chi^2/\text{d.o.f.}=287/303$; Figure 4), but requires a 7 times solar abundance of Fe. The three components all have different ionization parameters: $\log \xi = 1.986$ (with $r_{\text{in}} = 2.08 r_g$ and $r_{\text{out}} = 7.25 r_g$), 3.847 (with $r_{\text{in}} = 4.18 r_g$), and 1.722 (with

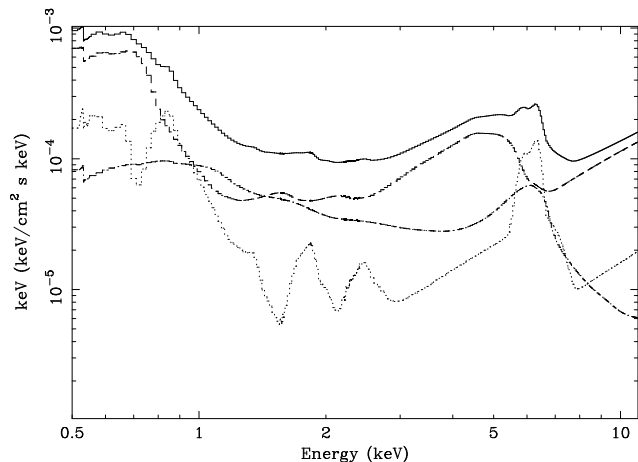


Figure 5. The three-reflector model that was successfully fit to 1H 0707–495. The solid line shows the total model, the dashed line plots the highly blurred but neutral inner reflector, the dot-dashed line shows the ionized reflector with $r_{\text{in}} = 4.81 r_g$, and the dotted line plots the outer neutral reflector with $r_{\text{in}} = 19.8 r_g$. These models do not contain any contribution from the incident power-law with $\Gamma = 2.35$.

$r_{\text{in}} = 19.8 r_g$). The last two reflectors had their outer radii frozen at $50 r_g$. The photon index and the inclination angle for all three components were fixed to have the same values. The best fit values were $\Gamma = 2.35$ and 18.2 degrees, respectively. The model is shown in Figure 5.

4 DISCUSSION

We have shown that the X-ray spectrum of 1H 0707–495 is well fitted by a reflection-dominated spectrum. The incident power-law is mildly steep with a photon index of 2.35. Furthermore, the model can completely account for the strong soft excess in this object by a combination of blurred emission lines and thermal emission from the irradiated blobs. The geometry envisaged for the source consists of a set of deep dense sheets or rings, orbiting the central black hole, between which hard X-rays are emitted. The fact that at least two reflectors are needed to provide a good fit to the data is not inconsistent with the model. There should be numerous rings or sheets in the centre of the disk with (as in the standard coronal picture) multiple hard X-ray sources active at any one time. The system is observed at sufficient inclination that the hard X-ray sources are not directly visible and only X-rays reflected from the sides of the dense matter are seen.

In fact, the model we have presented is a simplified picture of an intrinsically complex situation. In this respect, the interpretation of the fit parameters should be considered with some caution. In a more realistic situation, the reflection features will be broadened due to both relativistic effects and disc turbulence, so that parameters like r_{in} and r_{out} should not be taken at face value, but may be interpreted as the signature of the presence of different reproducers at different locations. Also, a range of ionization parameters is to be expected from the complex configuration we envisage, as a reflector would likely have an ionization gradient on its surface.

A consistent model for both the photon index of the input power-law and the reflection component is obtained if the opening angle of the gaps between the sheets or rings is less than 40 degrees and the whole disk inclination is about 20 degrees (Fig. 3 and Sect. 3). The metallicity is still required to be high (about 5–7

times the Solar value) but less than for other models. It is possible that the metallicity can be lowered if multiple reflection is included (this will have an approximately similar effect to squaring the reflection spectrum).

The spectral-independent variability of 1H 0707–495 (Boller et al. 2002) would be mostly due to changes in the brightness of the hard X-ray source causing the observed reflection components to vary. Additional variability may also arise from changes in the geometry of the system, with sheets or rings obscuring each other as they orbit the black hole. The geometry may also account for larger scale variations. When observed by *XMM-Newton*, 1H 0707–495 was about ten times fainter than in previous observations (Boller et al. 2002). This could be due to slight changes in the geometry and not necessarily a large change in intrinsic luminosity. If the hard X-ray source was previously more directly visible (say the opening angle of the sheets or rings was larger, or the hard X-ray emitting corona extended nearer to the disk surface) then the observed flux would have been larger. Indeed, the spectrum observed by *ASCA* when the flux was higher ($\Gamma \simeq 2.27$, Leighly 1999), is consistent with being the unobscured continuum emission peeking through the cold sheets.

It is possible that the model we have developed here for 1H 0707–495 has a wider relevance to Seyfert 1 galaxies. The reflection fraction can exceed unity if the disk is in the form of deep rings or sheets, and leads to an intrinsic hard power-law steeper than $\Gamma = 2$. MCG–6-30-15 has sometimes been observed with a spectral index of 2.1 or steeper (Vaughan & Edelson 2001; Shih, Fabian & Iwasawa 2001) and its strong iron line suffers far less variability than its continuum (Vaughan & Edelson 2001). This could be due to corrugations in its inner disk which may cause the reflection components to be stronger and more long-lasting than if the accretion disc was perfectly flat.

ACKNOWLEDGMENTS

ACF thanks the Royal Society for support. DRB acknowledges financial support from the Commonwealth Scholarship and Fellowship Plan and the Natural Sciences and Engineering Research Council of Canada. Based on observations obtained with *XMM-Newton*, an ESA science mission with instruments and contributions directly funded by ESA Member States and the USA (NASA).

REFERENCES

- Boller Th., Fabian A.C., Sunyaev R., Trümper J., Vaughan S., Balantyne D.R., Brandt W.N., Keil R., Iwasawa K., 2002, *MNRAS*, 329, L1
- Celotti A., Fabian A.C., Rees M.J., 1992, *MNRAS*, 255, 419
- Fabian A.C., Iwasawa K., Reynolds C.S., Young A.J., 2000, *PASP*, 112, 1145
- Guilbert P.W., Rees M.J., 1988, *MNRAS*, 233, 475
- Krolik J.H., 1998, *ApJ*, 498, L13
- Kuncic Z., Blackman E.G., Rees M.J., 1996, *MNRAS*, 283, 1322.
- Kuncic Z., Celotti A., Rees M.J., 1997, *MNRAS*, 284, 717.
- Laor A., 1991, *ApJ*, 376, 90
- Leighly, K. M., 1999, *ApJS*, 125, 317
- Lightman A.P., Eardley D., 1974, *ApJ*, 187, L1
- Malzac J., 2001, *MNRAS*, 325, 1625
- Malzac J., Beloborodov A.M., Poutanen J., 2001, *MNRAS*, 326, 417

- Merloni, A., Fabian, A. C., 2001, MNRAS, 328, 958
Nandra K., Pounds K.A., 1994, MNRAS, 268, 405
Nandra K., George I.M., Mushotzky R.F., Turner T.J., Yaqoob T.,
1999, ApJ, 523, L17
Petrucchi P.O., et al., 2000, ApJ, 540, 131
Pounds K.A., Nandra K., Stewart G.C., George I.M., Fabian A.C.,
1990, Nature, 344, 132
Pounds K.A., Done C., Osborne J.P., 1995, MNRAS, 277, L5
Ross R.R., Fabian A.C., 1993, MNRAS, 261, 74
Ross R.R., Fabian A.C., Young A.J., 1999, MNRAS, 306, 461
Shih D., Fabian A.C., Iwasawa K., 2001, MNRAS, submitted
Tanaka Y., et al., 1995, Nature, 375, 659
Turner N.J., Stone J.M., Sano T., 2001, ApJ, in press (astro-
ph/0110272)
Vaughan S., Edelson R., 2001, ApJ, 548, 694
Wardziński G., Zdziarski A.A., 2000, MNRAS, 314, 183
Zdziarski A.A., Fabian A.C., Nandra K., Celotti A., Rees M.J.,
Done C., Coppi P.S., Madejski G.M., 1994, MNRAS, 269, L55

This paper has been typeset from a T_EX/L^AT_EX file prepared by the author.